Novel approach to environment reconstruction in LADAR and HSI datasets

Dejan Nikic
The Boeing Company

Jason Wu
The Boeing Company

Paul Pauca
Wake Forest University

Robert Plemmons
Wake Forest University

Peter Zhang
Wake Forest University

ABSTRACT

A combination of shape and material data presented in a common data structure provides a platform for effective environment reconstruction and target detection. LADAR and hyperspectral image (HSI) data offer a vast amount of information, which can be redundant, that can completely reconstruct surfaces that generate reflections. These reflections are then captured by respective sensors. This paper discusses a physical approach, similar to electric field calculation of electron clouds, which can reconstruct the shapes captured by LADAR data, while a subspace representation is used to best approximate materials present in HSI data. The two data sets are merged by assigning the appropriate materials to the reconstructed surfaces. In this paper some of the benefits of this approach are discussed and experimental data is used to show the compression capability.

1. INTRODUCTION

LADAR and HSI data aggregation can be a powerful tool in target detection of remotely sensed environments. Unfortunately, both data types come with their own set of challenges. With LADAR data the sheer number of 3D points collected (approximately 1 million) presents a daunting processing task, even for modern computers. Traditional methods of Eucledian distance calculation between the points would require trillions of operations and are impractical for most cases where speed and efficiency are needed. HSI data has a very large number of spectral combinations (on the order of 256) that can be mixed, requiring a careful reconstruction of spectra. Because of the atmospheric effects and large stand-off distances of HSI sensors, noise and blur are presented in most HSI datasets. Algorithms for processing HSI data must account for noise and blur and correct the data before processing. These algorithms must also efficiently un-mix and interpret the resulting HSI spectral signatures. Because of the difference in resolution between LADAR and HSI data, there needs to exist a method that co-relates the two data sets. A method for classification and segmentation of the environment can be used to co-register the data. The data is based on the extents of the objects in the scene, allowing for large spectrally mixed HSI pixel integration on top of a higher resolution LADAR data set. In the model presented, the HSI data is not limited to the top surface of the object, but is also gathered along the height of the scanned surface. With this method, a combination of HSI sensors can be used (e.g., ground-based, different flight path) to generate material data for otherwise occluded surfaces.

Research supported by National Geospatial Intelligence Agency under contract HM1582-10-C-0011 PA 12-381

2. ENVIRONMENT RECONSTRUCTION

In order to faithfully represent the physical properties of a remotely sensed environment, a model is developed to represent the shape of the objects present and apply spectral responses to the surfaces that make up the shape.

2.1 Shape reconstruction

Using LADAR data, a shape is reconstructed using the implicit geometry (IG) method [1]. Three functions are applied to the rectangular mesh that contains all of the data points. Each function provides a unique field, each with its own set of advantages for different applications. Let Ω denote the observed space or test site. Given a set of LADAR sampling points $P \subset \Omega$ collected, three different types of fields can be calculated using the functions described below.

2.1.1 Population function

Computationally fastest of all, $\mathcal{O}(N)$the population function, counts the number of LADAR data points belonging to a specific mesh cell. A field that is generated by the population function is localized to an individual cell. This function does not depend on the lidar points that lie outside of the IG cell. The population function is advantageous in applications where rapid processing is required and where a distribution of LADAR point cloud is important.

2.1.2 Distance function

The distance function $d(\omega)$ for any $\omega \in \Omega$ to the data point set P is defined as the solution of the Eikonal equation (1).

$$\begin{aligned} |\nabla d(\omega)| &= 1 \\ d(\omega) &= 0 \quad if \quad \omega \in \Omega \end{aligned} \qquad (1)$$

Unlike the population function, distance function values are computed by looking at the LADAR points contained in a region of interest defined by a radius. In general, the distance function offers a superior rendering capability when compared to the population function. The computation time for distance function is $\mathcal{O}(N)$, the same as the population function — but there is an additional computational penalty caused by extra calculation of the surrounding mesh cells. In our studies, the distance function has been 5 to 10 times slower than population function.

2.1.3Validity function

For any given point $\omega \in \Omega$, the validity of this position is defined (2), where p is a data point in P and f could be a hardware-dependent point-spread function (PSF) or a user supplied distribution function.

$$v(\omega) = \sum_{p \in P} f(\omega - p) \qquad (2)$$

For our model, the validity function closely resembles the electric field calculation because the imposed PSF resembles $\frac{1}{r}$ or $\frac{1}{r^2}$ depending on the application and raw data properties, where r is the distance between the cell node and LADAR point. Similar to the distance function, the LADAR data points contained in neighboring cells that are defined by a radius affect the validity function. The computation time of the validity function is comparable to that of the distance function.

2.1.4 Surface rendering

For all three functions the underlying shape of the sensed object can be reconstructed by rendering an iso-surface of the IG field [2]. For a given threshold T, we then compute the isosurface $S \subset \Omega$ such that for any $\omega \in S, v(\omega) = T$.

The value of T is chosen based on the function used to generate the IG field. The rendering process is same for all three functions described above, but the choice and span of T varies based on the function. We implemented our renderings based on the Marching Cubes method [3]. Surface rendering is used only for display purposes and has no direct effect on the algorithms that analyze the data. Surface rendering is just one of the many applications that the IG fields can be used for.

2.2 Material reconstruction

Given a HSI data cube $f(x, y, \lambda)$ we seek a sparse representation of the two spatial dimensions shown in (3), where $s(\lambda)$ is the spectral signature and $u(x, y)$ is the characteristic function [4]. Using this type of representation the HSI data is compressed, unmixed and easier to interpret.

$$f(x, y, \lambda) = \sum_{i=1}^{L} u_i(x, y) s_i(\lambda) \qquad (3)$$

2.2.1 Total variation (TV) model

A piecewise constant segmentation model (4), where f_j is the j-th slice of the hyperspectral cube, s_{ij} is the reflectance of i-th spectrum at j-th wavelength and τ is the regularization parameter, can be extended to HSI data. Applying the total variation model to HSI data combines all slices while minimizing the total variation of the membership function, which only resides on the two spatial dimensions, independent from spectral slices.

$$E(u, s) = \sum_{i=1}^{L} \int_{\Omega} |\nabla u_i| dxdy + \sum_{i=1}^{L} \frac{\tau}{2} \int_{\Omega} \frac{1}{m} \sum_{j=1}^{m} (f_j - s_{ij})^2 u_i^2 \, dxdy \qquad (4)$$

One major advantage of the total variation model is that in the presence of a noise or blurring, the model can be coupled with a de-blurring and de-noising model (5), where f_0 is the observed HSI data and γ is the regularization parameter [5]. For the cases where the blurring operator h is well characterized, the blur can be eliminated completely.

$$E(u, s) = \sum_{j=1}^{mL} \int_{\Omega} |\nabla f_j| dxdy + \frac{\gamma}{2} \int_{\Omega} (h \cdot f - f_0)^2 dxdy + \sum_{i=1}^{L} \int_{\Omega} |\nabla u_i| dxdy + \sum_{i=1}^{L} \frac{\tau}{2} \int_{\Omega} \frac{1}{m} \sum_{j=1}^{m} (f_j - s_{ij})^2 u_i^2 \, dxdy \qquad (5)$$

2.3 Combination of shape and material information

Given the IG approach, various properties can be assigned to individual cells. A single spatial location in the IG mesh can hold population, validity, and distance field values alongside the HSI data characteristic function coefficient.

Before assigning HSI characteristic function coefficients to their respective cells, a data structure containing spectral signatures needs to be generated. Once the spectral signatures are connected with the IG cells by characteristic function coefficients, a full representation of geometry and material data is presented. A final data structure (6) will contain the IG field values as well as the characteristic function coefficients, and additional data can be added as well. In the current implementation, available RGB data can be added.

$$IG(x, y, z) = \{p, d, v, u\} \qquad (6)$$

To consolidate HSI and LADAR data, each mesh is assigned values of the three IG functions (population, distance, and validity) and the HSI coefficient u_i. Spectral signature $s_i(\lambda)$ is stored in a data structure accessible by the IG mesh. Since the IG mesh is a 3D structure and the characteristic function $u_i(x, y)$ is in 2D space, we project u_i over the IG mesh. Depending on the application, the u_i can be assigned just to the bottom row of mesh cells, all mesh cells belonging to particular (x,y) location, or any other combination.

Currently, data from only one pose is available. But with the meshed domain a variety of sensors can be combined to give data from different viewing angles. This increases the fidelity and fills in areas that might be occluded. For instance, ground-based HSI and LADAR sensors can obtain data for the sides of objects that is generally not available from sensors that are flown directly above the scene.

3. APPLICATON TO GULFPORT LADAR AND HSI SCENE

A data set was acquired by a team led by Professor Paul Gader from the University of Florida Department of Computer and Information Science and Engineering. The data was captured over the campus of the University of Southern Mississippi (USM) in Gulfport, Mississippi. LADAR and HSI data were acquired concurrently and co-registered. The HSI data, with bands from $0.454\ \mu m$ to $0.719\ \mu m$, was acquired by a CASI sensor. Out of the original 72 bands ranging from $0.4\ \mu m$ to $1.0\ \mu m$, 58 bands were selected for higher signal to noise ratio.

From the data selected, a section that spans 320 by 360 meters was segmented for testing. This area encompasses a center of the USM campus and shows numerous urban features (e.g., buildings, roads, trees, vehicles), as shown in Fig. 1.

A LADAR data set with approximately 183,000 LADAR points, Fig. 2, was used to generate the IG validity field. A regular rectangular mesh with one meter resolution was used. The total computation time of the validity field was approximately 0.5 seconds. The iso-surface was generated using the IG validity field Fig. 3. The cut-off value of the iso-surface was chosen manually to generate a plot that best represented the USM campus scene.

HSI portion of the data was processed using a TV method with m=7 as defined in (4). Fig. 4 shows a subset of representative spectral returns. The characteristic function $u(x, y)$ that was obtained using the total variation method was combined with the validity field. The combination of the characteristic function and the validity field resulted in a full representation of the USM scene in Fig. 5.

Fig. 1. Areal view of USM campus in Gulfport, MS [6]

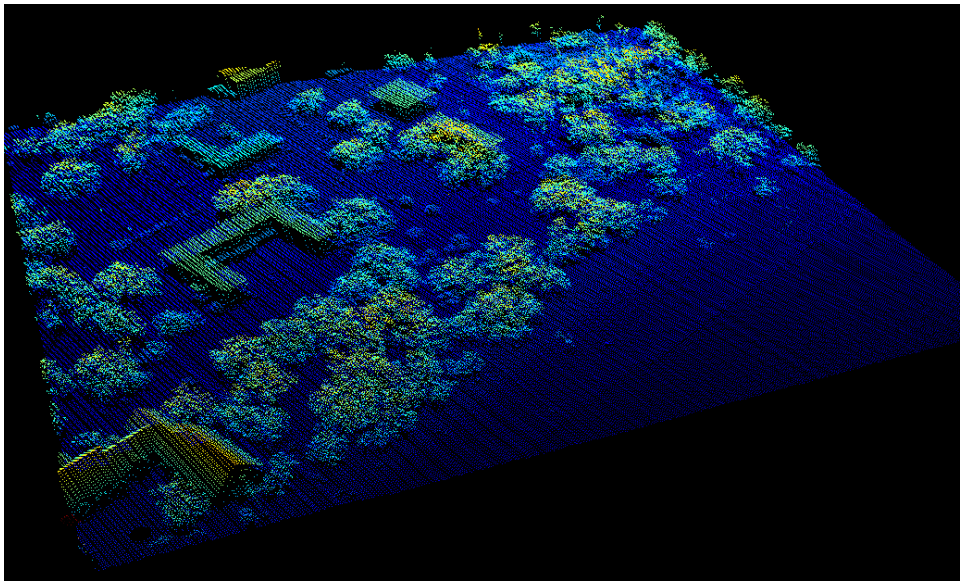

Fig. 2. LADAR data of the USM campus, with false color based on height.

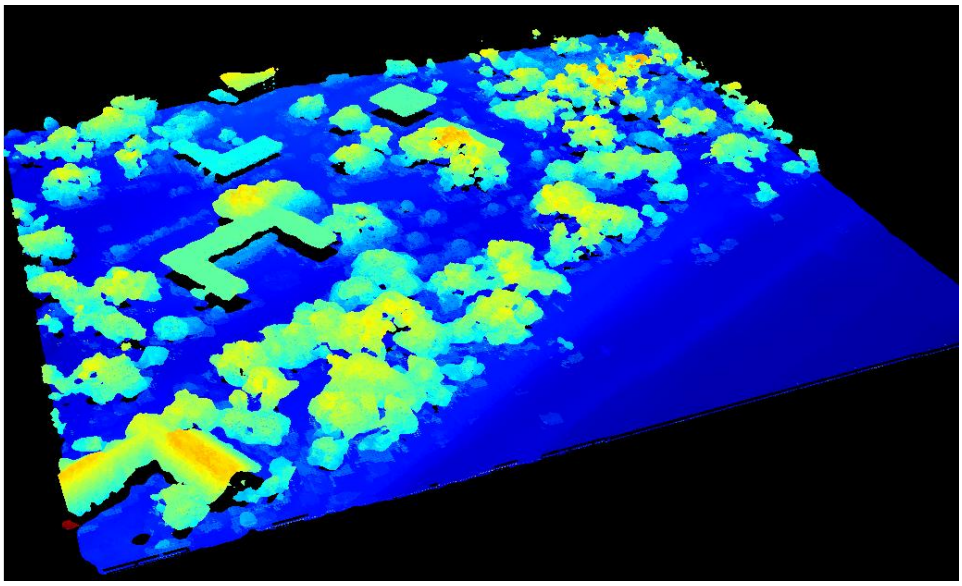

Fig. 3. Iso-surface plot of IG validity field, with false color based on height.

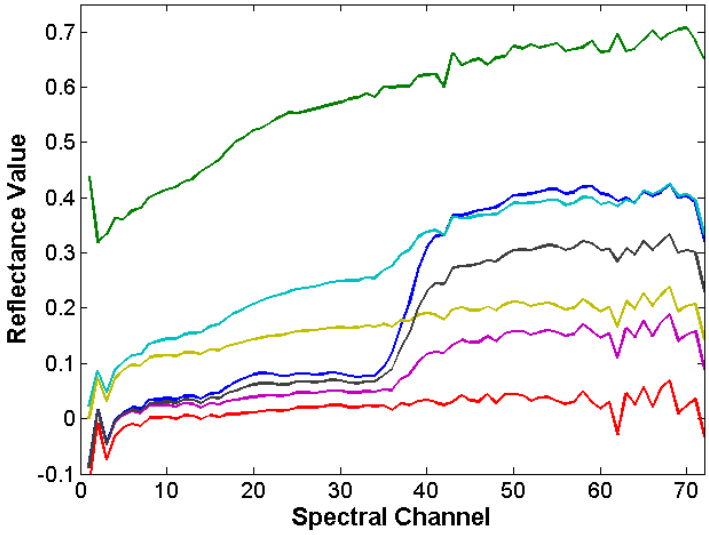

Fig. 4. Spectral returns of the sparse representation of HSI data for 7 spectral signatures

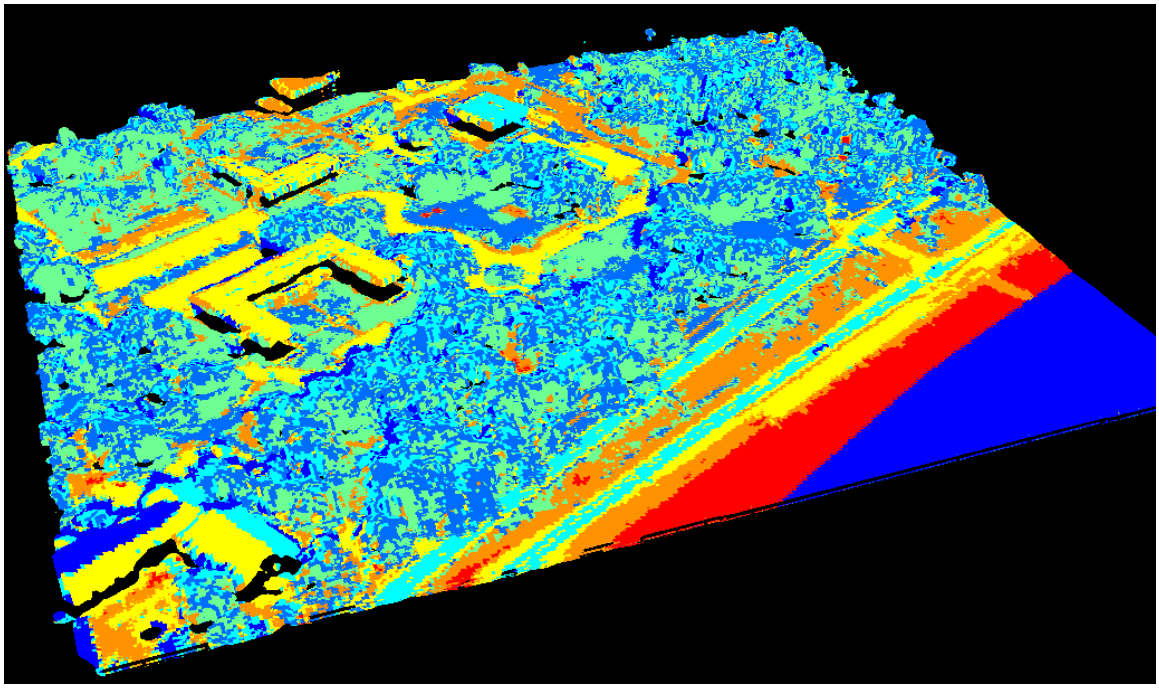

Fig. 5. Combination of IG validity field iso-surface and characteristic HSI function, where colors represent the different spectral returns shown in Fig. 4.

4. FUTURE WORK

Using the described data fusion model one can extract fused data and use it for object detection, classification, and clustering. Our future work will center on interrogating this fused data. An extension of the model presented here will be used to effectively classify and cluster mixed LADAR and HSI data. Application of a mixed dataset should provide superior classification capabilities with reduced false alarms and an increased probability of detection. Similarly, our future object detection work will use rule sets to interrogate the scene and find patterns that define a particular object. We will investigate the suitability of this approach for complex objects such as trees, vehicles, and buildings.

5. CONCLUSION

The described algorithms and methods for combining LADAR and HSI data have provided great utility in combining the datasets. After combining, the new data structure can store multiple datasets from different sensing platforms and poses necessary to obtain a complete environment reconstruction.

6. REFERENCES

1. B. Merriman, M. Kang, H.K. Zhao, and S. Osher., "Implicit and nonparametric shape reconstruction from unorganized data using a variational level set method.," Computer Vision and Image Understanding, vol. 80, pp. 295– 314, 2000.

2. R. Fedkiw and S. Osher., "Level set methods: an overview and some recent results," Journal of Computational Physics, vol. 169, pp. 463–502, 2001.

3. Harvey E. Cline and William E. Lorensen, “Marching cubes: A high resolution 3d surface construction algorithm,” Computer Graphics, vol. 21, pp. 4, 1987.

4. R. Plemmons, S. Prasad, F. Li, M. Ng, and Q. Zhang., “Hyperspectral image segmentation, deblurring and spectral analysis for material identification,” in SPIE Symposium on Defense, Security, and Sensing, 2010.

5. D. Kittle, D. Brady, Q. Zhang, R. Plemmons, and S. Prasad., “Joint segmentation and reconstruction of hyperspectral data with compressed measurements,” Applied Optics, vol. 50, pp. 4417–4435, 2011.

6. GOOGLE EARTH, 30°21’06.19” N 89°08’07.59” W, Guflport, MS, 12/25/2011